

<https://doi.org/10.1038/s40494-025-02245-1>

Ancient waterlogged ivory: tracing its origin through DNA analysis and spectrometric methodologies

Check for updates

Marina Costa^{1,2}, Cláudia S. L. Vicente², Margarida Espada², Jorge M. S. Faria³, Jorge Ginja Teixeira¹, José Bettencourt^{1,4} & Dora Martins Teixeira¹✉

Underwater archaeological excavations at a shipwreck located in the port of Horta (Azores), uncovered a cargo of elephant ivory tusks, likely from a British merchant vessel that sank in the early 18th century. Since the ship's route remains uncertain, determining the ivory's provenance was essential for reconstructing its historical and commercial context. A multidisciplinary analytical approach combining X-ray fluorescence (XRF), Fourier-transform infrared spectroscopy (FTIR), and ancient DNA (aDNA) analysis was employed. FTIR spectra displayed a typical dentin profile, with Infrared Splitting Factor values (3.45–3.58) indicating moderate diagenetic alteration but overall good preservation. XRF results reflected both biogenic composition and post-depositional effects, with copper absence in two samples possibly linked to biological variation. Molecular analysis identified an African origin for the ivory, probably obtained during a stopover at an African port, supporting the initial archaeological hypothesis. This study also highlighted that EDTA removal after samples decalcification improves DNA extraction efficiency.

In the 17th century, the Azores archipelago played a crucial role in Atlantic trade routes due to their strategic mid-ocean location, making them an essential stopover for ships traveling between Europe, Africa, and the Americas. Positioned along the return path of the prevailing westerlies, the Azorean ports offered a safe and reliable place for ships to resupply with fresh water, food, and repairs after long transatlantic journeys. These became important logistical hubs for merchant and military fleets, especially for those carrying valuable cargo such as sugar, silver, tobacco, and ivory. The Azores were not only a physical landmark in navigation but also a vital connection in the economic and imperial networks of the early modern Atlantic world. The diversity of shipwrecks from the 17th and 18th centuries found in the Azores highlights the islands' strategic position in the Atlantic, with remains of Portuguese, Spanish, British, Dutch, and French vessels that reflect a wide range of maritime activities, including transatlantic trade, military operations, privateering, and colonial expeditions, underscoring the Azores' vital role as a stopover, refuge, and battleground in early modern global navigation¹.

The Horta seaport (Faial, Azores, Portugal) became a crucial port of call for British ships involved in transatlantic trade^{1–3}. In 2008, the remains of a historically important shipwreck were found [Baía da Horta 1 (BH-001)]^{3,4}

that contained a rich variety of artifacts, e.g., preserved glass bottles, stoneware, and ceramics, dating to the early 18th century. Also, a cargo of kaolin pipes revealed the Manby's family mark, whose production in London is well-documented in the first half of the 18th century, suggesting its British origin^{5,6}. The most significant discovery in BH-001 was 100 elephant ivory tusks in excellent state of preservation, due to the underwater environment with low oxygen levels, stable temperatures, and protective sediment layers that slow decay and protect them from damage and biological degradation⁷. In the late 17th and early 18th centuries, ivory was highly valued raw material for the production of luxury items^{4,5,8}. Sunken ivory cargoes were found on several shipwrecks related to the Atlantic trade, such as the *Henrietta Marie* (Florida, United States, 1700), the *Fredensborg* (Tromøy, Norway, 1768), or the *Saint-Quay-Portrieux* (Brittany, France, c. 1700)^{9–12}. Ivory as cargo has as well been documented in shipwrecks involved in the Cape Route, suggesting that a large part of the African ivory brought to Europe was re-exported to Asia. In modern deposits, ivory tusks were found in two shipwrecks from the Portuguese India Run - *Oranjestad* (Namibia - first half of the 16th century), *IDM3* (Mozambique - early 17th century) and in two from the Dutch East India Company (VOC) - *Vergulde Draeck* (Australia - 1656) and *Risdam* (Malaysia - 1727)^{13–15}. This

¹HERCULES Laboratory & Chemistry and Biochemistry Department of Science and Technology School, University of Évora, Évora, Portugal. ²MED–Mediterranean Institute for Agriculture, Environment and Development & CHANGE—Global Change and Sustainability Institute, Institute for Advanced Studies, and Research, University of Évora, Évora, Portugal. ³INIAV, National Institute of Agricultural and Veterinary Research, Av. da República, Quinta do Marquês, Oeiras, Portugal.

⁴CHAM–Center for the Humanities and History Department, FCSH, Universidade NOVA de Lisboa, Lisbon, Portugal. ✉e-mail: dmt@uevora.pt

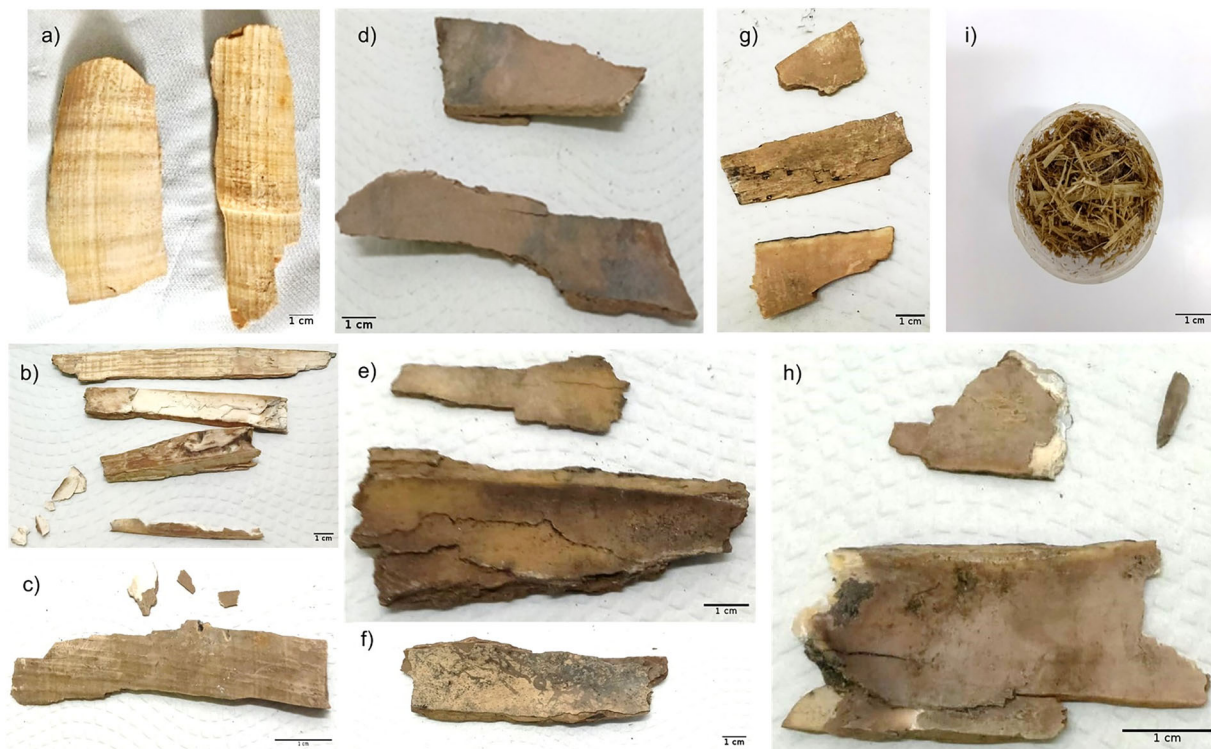


Fig. 1 | Ivory tusks samples from the BH-001 shipwreck (Faial, Azores, Portugal). Macroscopic view of the archaeological submerged ivory samples analysed: **a** ACO and PHA; **b** BHA_35; **c** BHA_41; **d** BHA_34; **e** BHA_37; **f** SR; **g** BHA_59; **h** BHA_49 and an example of contemporary elephant faecal sample used (**i**).

context complicates the search for the provenance of the BH-001 vessel. Even if most of the excavated finds originate from the Atlantic, especially Europe, the geographic provenance of the ivory tusks from BH-001 is still under scrutiny^{4,5,8}.

Analytical chemistry allied to molecular biology offer a complementary approach to study ancient, waterlogged ivory tusks. Chemically, ivory is composed of organic material (i.e., collagen, elastin, and lipids) within a non-stoichiometric matrix of carbonate-containing apatite, similar to hydroxyapatite ($\text{Ca}_{10}(\text{PO}_4)_6(\text{OH})_2$)^{16,17}. The ions in this inorganic substance can partially substitute during an elephant's life or even after death, while the organic material naturally degrades post-mortem. The identification of elephant tusks has mostly relied on morphological analysis of the characteristic Schreger lines and angles in ivory^{18,19}. Schreger lines are cross-hatched visual patterns observed in transverse and longitudinal sections of ivory, resulting from the periodic orientation of dentinal tubules within the tusk structure²⁰. Despite its usefulness this method is very often inconclusive by itself.

Recent advances in analytical methods, such as X-ray fluorescence (XRF), Fourier-transform infrared spectroscopy (FTIR), isotopic composition analysis techniques e.g., LA-ICP-MS (laser ablation inductively coupled plasma mass spectrometry) or IR-MS (isotope ratio mass spectrometry), along with ancient DNA sequencing, could bring significant progress to this research area^{21–24}.

For example, XRF spectrometry allows easy determination of an ivory sample's surface elemental composition²². Portable XRF devices allow simple, non-destructive, and quick multi-elemental analysis of ivory items^{25–27}. The Ca/P ratio, based on ivory's primary elements, calcium and phosphorus, helps differentiate ivory from similar materials and can also aid in identifying its geographic origin and elephant species^{25–27}.

The aim of this study was to characterize the elephant ivory recovered from the shipwreck BH-001, dating from the 18th century, in the Azores (Portugal), using a multi-analytical approach to more accurately identify the elephant species that originated the ivory in this shipwreck. Thus, this study can potentially confirm this ship's connection to Atlantic navigation and

open research perspectives that go far beyond the regional historical context of the Azores.

Methods

Ivory tusks

Ivory tusks, submerged for ca. 300 years, were recovered from the archaeological site BH-001 (Faial, Azores, Portugal) and preserved in water tanks at the Horta Museum (city of Horta in Faial Island) to prevent degradation. Nine tusk samples (Fig. 1a–h) were kindly provided to be used in this study. Additionally, two samples of faeces from Asian elephant (*Elephas maximus*) (Fig. 1i) and African savanna elephant (*Loxodonta africana*), were kindly provided by Terra Natura (Benidorm, Spain) and the Lisbon Zoo (Lisbon, Portugal) respectively, to be used as controls for the molecular biology studies to identify the elephant species.

Pre-treatment of ivory samples

Ivory tusk samples were cut into small pieces (2 cm) using an electric circular saw (Struers, Discoplan-TS) and superficially pulverized using a Dremel® sanding tool. The cleaned samples were then rinsed with a 10% (v/v) sodium hypochlorite solution and then with sterile water. After drying for 24 h at 37 °C, cleaned ivory pieces were grounded for 5 min at 500 r.p.m. in a ball mill (Retsch Planetary Ball Mill PM 100 PM100, Germany). Processed samples were finally stored at room temperature in sterilized 50 mL tubes before analysis.

Fourier-transform infrared spectroscopy (FTIR)

The FTIR analysis was performed using a portable Bruker ALPHA spectrometer (©Bruker Corporation, Billerica, USA) in absorbance mode, controlled by OPUS 6.5 software (©Bruker Corporation, Billerica, USA), and coupled with a single-reflection diamond attenuated total reflectance (ATR) module. The powdered material was analysed at room temperature, and three spectra were taken in the 4000–375 cm^{-1} range with a resolution of 4 cm^{-1} and 128 scans per spectrum for each measurement. Prior to each analysis, a background spectrum of the air was always collected to remove

atmospheric interferences. The spectra were baseline corrected and normalized after peak measurement.

X-ray fluorescence (XRF)

For XRF, 22 disinfected non-powdered ivory fragments were used per sample. Analysis was performed with a handheld/portable energy dispersive X-ray fluorescence spectrometer Bruker Tracer III- SD (Bruker AXS, Billerica, USA) equipped with a rhodium X-ray tube and a X-Flash® SDD (silicon drift detector) to determine the elemental composition (major, minor and trace elements) of the ivory fragments with $Z \geq 14$ (Si). The spectra acquisition was performed with Bruker S1PXRF software (version 3.8.30). The operation conditions were set to 40 keV, 30 μ A, 180 s of acquisition time, and without filter or vacuum. To get representative data, each ivory fragment was analysed at random spots in its surface (approximately 10 mm in diameter).

The spectra analysis was performed using Bruker S1PXRF software and the Bruker ARTAX software (version 5.3.15.1). Due to the heterogeneity of sample physicochemical surface (e.g., uneven analysis areas, density variations, and differences in elemental composition) and in the absence of an independent method for absolute quantification, no attempt was made to quantify elements such as calcium, phosphorus, and others.

The relative elemental composition was obtained from 121 XRF spectra analysed by the Bayesian deconvolution method using ARTAX software, which provides the net photon counts emitted by a given element, the net intensities. Considering that X-ray intensity and analyte concentration are generally non-linearly correlated, it can be assumed that the net intensities are proportional to the elemental concentrations. These net intensities correspond to the area under the spectral peaks of each element, corrected for inter-elemental effects, background radiation, escape peaks, and sum peaks.

Sample decalcification and cleaning for DNA extraction

The powdered ivory samples were decalcified with 1 mL of 0.5 M EDTA solution (pH 8.5) for 1 h at 56 °C and 400 r.p.m., followed by centrifugation at 9000 r.p.m. for 10 min. The remaining pellets were washed twice with 1 mL sterile distilled water and leftover ethylenediaminetetraacetic acid (EDTA) was removed with 0.5 M magnesium nitrate, since this reagent can negatively impact downstream applications such as DNA extraction and PCR amplification²⁸.

Total DNA extraction and PCR amplification

Total DNA extraction of the decalcified ivory samples was performed with the commercial kit DNeasy® PowerSoil® Pro Kit (Qiagen) following the manufacturer's instructions. A short fragment (116 bp) of the mitochondrial cytochrome b gene (*cyt b*) was used for elephant identification, using the L15123/H15240 primer pair²⁹. Samples were amplified by PCR using 1U Platinum™ Taq DNA Polymerase High Fidelity (Invitrogen, ThermoFisher Scientific), 1 ng of DNA template, 0.2 μ M of forward and reverse primers, 0.2 mM of dNTP mix, 1x High Fidelity Buffer and 2.0 mM of MgSO₄, for a final volume reaction of 25 μ L. The amplification programme was the following: initial denaturation 95 °C for 3 min, followed by 40 cycles of 30 s at 94, 51 and 72 °C, followed by final extension at 72 °C for 20 min²⁹. The PCR products were analysed by 1.5% agarose gel electrophoresis and purified using MinElute® Gel Extraction Kit (Qiagen, Hilden, Germany). Whenever possible, PCR products were cloned using pCR™8/GW/TOPO™ TA Cloning Kit with One Shot™ TOP10 *E. coli* (Invitrogen, Thermo Fisher Scientific), according to the manufacturer's instructions. This step enabled the generation of homogeneous clonal DNA templates, improving the accuracy and clarity of subsequent Sanger sequencing results.

Following confirmation of the target PCR product, plasmid DNA was extracted using the NZYMiniprep kit (NZYtech, Lisbon, Portugal). Sequencing was performed by STABVIDA (Costa da Caparica, Portugal).

Sequence analysis and phylogeny inference

Raw sequences were analysed, manually trimmed using BioEdit v7.2.5³⁰ and deposited in NCBI GenBank. Sequences were used as query at NCBI GenBank for preliminary identification using BLAST tool (<https://blast.ncbi.nlm.nih.gov/>). Sequences from closely related species were retrieved from the database for the phylogenetic analysis. Multiple sequence analysis was conducted using MAFFT v7.0³¹, trimmed with trimAL v.1.4.1³². The phylogenetic tree was reconstructed using the Maximum likelihood method and the best fitting model selected in the Model Testing plugin from CLC Main Workbench 24.0 software (QIAGEN, Aarthus A/S). The robustness of the phylogenetic tree was supported by 1000 bootstraps.

Results

Spectrometric profiling

The physical and chemical properties of elephant ivory are strongly related to the composition and size of the cHAP crystals, as well as to the collagen content. For archaeological ivory, the different diagenetic processes over time can significantly alter the original constituents, namely, the cHAP crystals and the collagen matrix^{33,34}. FTIR spectroscopy (in either transmission or ATR mode) reveals the chemical composition of elephant ivory and monitor changes over time, this technique has been widely used to evaluate crystallinity changes and the loss or degradation of organic material in ancient ivories^{35,36}. FTIR has controversially been proposed as one of the few analytical techniques capable of distinguishing African from Asian ivory^{37,38}.

The FTIR-ATR spectra, obtained for the nine ivory samples presented a similar profile, characteristic of mineralised collagen (Fig. 2). The main bands of the phosphate, carbonate and amide group clearly stood out. The differences observed in the assigned bands when compared to previous studies, were due to the age of the samples as well as the waterlogged environment in which the items were discovered^{35,39–41}. Besides the band assigned to the ν_3 (CO_3^{2-}) vibration, three bands were observed between 1720 and 1170 cm^{-1} , that are characteristic of collagen amide groups. The band ascribed to the amide I functional group (at 1643 cm^{-1}), and to a lesser extent the amide II band (at around 1540 cm^{-1}), may include an indeterminate contribution from water (due to its bending vibration near 1630 cm^{-1}), creating some uncertainty about the presence of these functional groups^{42,43}. The amide III band (at around 1240 cm^{-1}), although with a very weak intensity when compared to the other two, is not affected by any water-related absorption (Fig. 3). Therefore, its detection indicates that these functional groups and their associated organic substances remain in the ivory matrix (mainly dentin), suggesting relatively low diagenetic degradation. To corroborate this assumption and evaluate the relative state of preservation of these archaeological samples, several commonly used crystallinity and preservation indicators were selected and assessed. These include the infrared splitting factor (IRSF, also referred to as the crystallinity index or CI), the carbonate/phosphate ratio (C/P or $\text{CO}_3^{2-}/\text{PO}_4^{3-}$)^{35,36}, the amide I/phosphate ratio (AmI/P or $\text{AmI}/\text{PO}_4^{3-}$), and the amide I/amide II ratio (AmI/AmII)⁴².

The IRSF values, calculated by summing the heights of the 600 cm^{-1} and 560 cm^{-1} absorption bands and dividing by the height of the valley between them (with a baseline between approximately 470 and 670 cm^{-1}), provide a rough measure of phosphate crystal structure and composition in natural bioapatites^{16,35,36,44}. Generally, IRSF values increase with recrystallization and the loss of structural B-type carbonate (both increases the crystal order), as well when the entire matrix loses organic material^{35,36,44}. For archaeological unprocessed/raw dentin samples (typically what remains of ancient elephant tusks), IRSF values between 2.98 and 3.60 are considered indicative of good preservation, while values above 4.0 suggest significant structural and compositional alteration³⁶. Most of the ivory samples analysed here presented IRSF values ranging from 3.45 to 3.58, with one sample (BHA_SR) slightly exceeding this range at 3.65. Therefore, according to this index, the samples appear to be relatively well preserved, albeit with some degree of alteration.

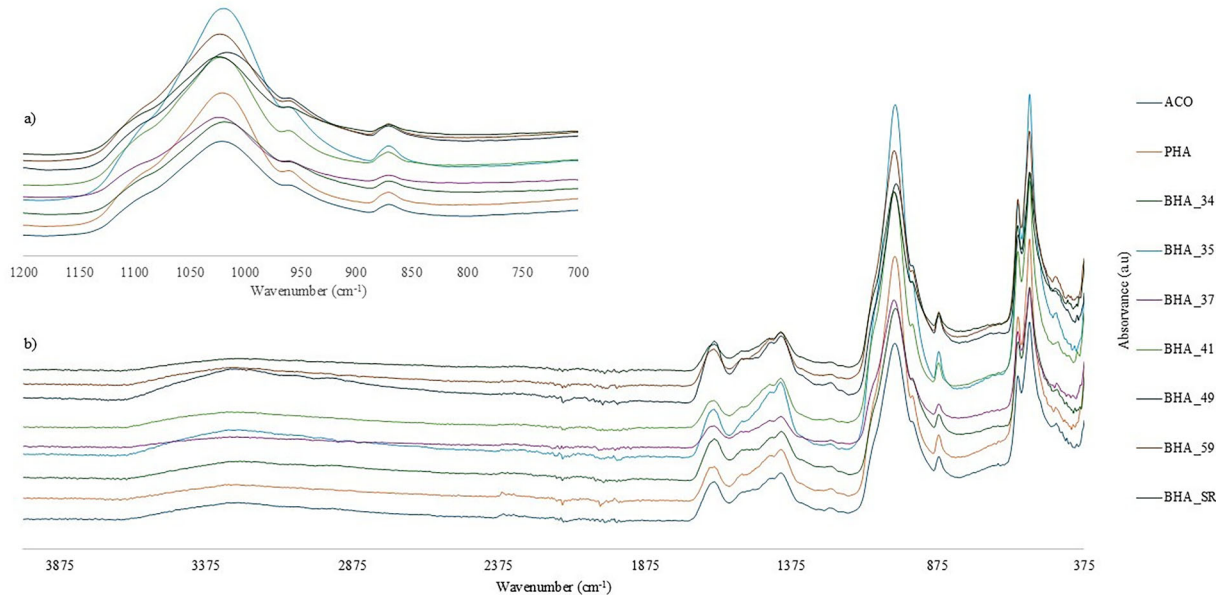


Fig. 2 | FTIR spectra of the nine elephant ivory samples from the BH-001 shipwreck. Panel (a) shows the region between 1200 and 700 cm^{-1} , emphasising the main phosphate and carbonate vibrational bands of hydroxyapatite. Panel (b)

presents the full FTIR spectra of the nine ivory samples (ACO, PHA, BHA_34, BHA_35, BHA_37, BHA_41, BHA_49, BHA_59, and BHA_SR).

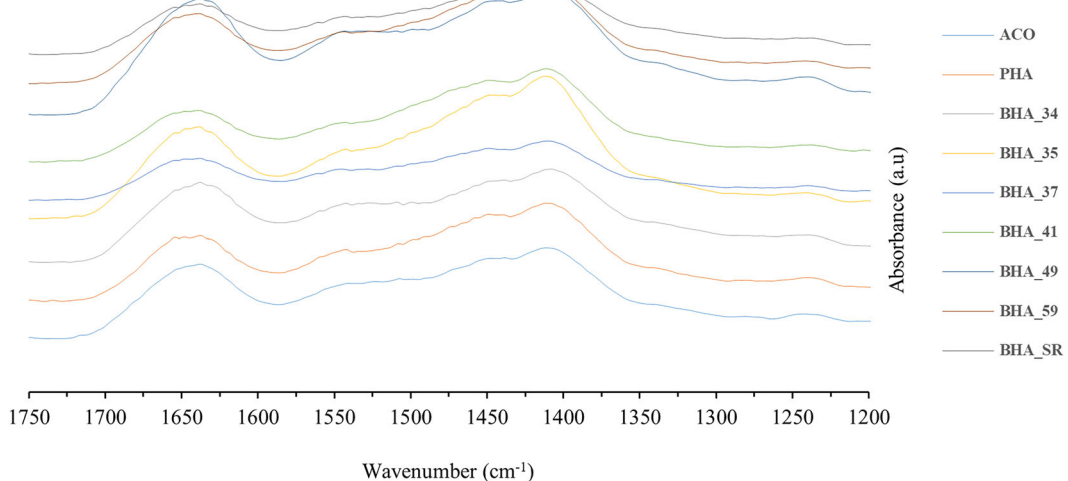


Fig. 3 | FTIR spectrum between 1750–1200 cm^{-1} , revealing the amide I (1643 cm^{-1}), II (1546 cm^{-1}) and III (1237 cm^{-1}) bands, suggesting relatively low deterioration of the samples.

The carbonate to phosphate ratio (C/P), calculated using the ratio of absorption heights at 1409 cm^{-1} and 1021 cm^{-1} (assuming an appropriate baseline), decreases as carbonate is partially or fully removed, reflecting an increase in crystal order. For the studied samples, C/P values range from 0.23 (sample BHA_SR) to 0.36, falling within the expected range for well-preserved archaeological dentin³⁶. A general trend was observed wherein decreasing C/P values correlate with increasing IRSF values (see Table S1 and Fig. S1A in the Supplementary Information), i.e., samples with lower alteration tend to show higher C/P ratios and lower IRSF values³⁵. The amide I/phosphate ratio (AmI/P, calculated by dividing the intensity of the amide I band at 1650 cm^{-1} by the PO_4^{3-} band at 1021 cm^{-1}) and the amide I/amide II ratio (AmI/AmII, calculated from the amide I intensity at 1650 cm^{-1} divided by that of the amide II band at 1550 cm^{-1}), are considered rough indicators of collagen content and its relative preservation quality, respectively. The AmI/P values among the samples ranged from 0.12 to 0.33, while the AmI/AmII ratios clustered around 1.6 ± 0.1 . In addition, despite some difference observed between the intensities of amide I and amide II bands among the

samples, a good linear correlation was obtained between the intensity of amide II and amide I bands (Table S1 and Fig. S1B, in Supplemental information file). The AmI/P values suggest varying collagen content across the samples, with three (BHA_49, BHA_34, and ACO) exhibiting higher values (see Table S1 and Fig. S1C).

Compared to the reference values of AmI/P ratios ascribed for fresh and modern bones (> 0.1), these samples show AmI/P ratios indicative of good collagen preservation⁴². On the other hand, the AmI/AmII values suggest that, despite the retained collagen content, the molecular structure of the collagen has undergone hydrolysis or denaturation, processes that typically result in higher AmI/AmII ratios. Unaltered collagen matrices would be expected to show lower AmI/AmII values. Remarkably, the three samples with the highest AmI/P values (BHA_49, BHA_34, and ACO) are also those with the highest C/P values and the lowest IRSF values (see Table S1 and Fig. S1D in the Supplementary Information), denoting that the samples with higher collagen content were also the ones where the recrystallization and loss of structural B-type carbonate were less pronounced.

Although the shoulder around 1100 cm^{-1} has been proposed as a distinguishing feature in FTIR spectra between African and Asian elephant ivory^{21,45–47}, this distinction remains inconclusive. Several studies have shown that this spectral feature is not exclusive to African ivory, having also been observed in Asian specimens^{37,38}. Moreover, variations in spectral profile, particularly within the $1096\text{--}1083\text{ cm}^{-1}$ region, may result from differences in signal intensity, diagenetic alteration, burial conditions, and the anatomical region sampled^{23,48}. These factors can affect the vibrational bands associated with carbonated hydroxyapatite, whether integrated within the apatite lattice or associated with the surrounding organic matrix. As such, while FTIR provides valuable insights into structural and compositional changes, it should not be used in isolation for taxonomic attribution. In particular, the assumption that crystal size differences in cHAP are sufficient to differentiate African from Asian ivory lacks consistent empirical support. When possible, complementary techniques such as genetic analysis should be employed to strengthen species identification. The corresponding

spectral characteristics, functional groups and vibration modes are summarized in Table 1.

The XRF spectra acquired for PHA and BHA_34 are representative of the remaining samples, and showed that the major elements were Ca, P, Fe, and Sr (Fig. 4). As minor elements, it was possible to identify Ni, Mn, Zn, S, and Br, and lastly Cu, but in only seven samples. PHA and ACO samples did not present a significant presence of this metallic element (see for instance Fig. 4, wherein the BHA_34 spectrum presents a well-defined copper peak and PHA does not). In some samples, trace amounts of As, Pb, Cr, and Y were found. In general, none of the elements is unexpected for elephant ivory samples. Elements like Zr or Hf, that can be used as discriminating or reference elements, were not seen above detection limits in any of our 121 XRF spectra^{38,46}.

The elements Ca and P, naturally occurring in ivory were easily identified in all spectra. Using the operating conditions detailed, the ratio between Ca ($K_{\alpha 1}; K_{\alpha 2}$) and P ($K_{\alpha 1}; K_{\alpha 2}$) net intensities peaks was 16.5 ± 0.6 . Between samples, between sections from the same sample, or even at dif-

Table 1 | Spectral characteristics, functional groups and vibration modes ascribed to the absorption bands shown in the FTIR spectra

Wavenumber (cm^{-1})	Functional group	Vibration mode	References
3600 - 3300	$\text{OH}, \text{H}_2\text{O}$	Stretching	17,23,38,43,68–70
1643	Amide I	$\text{C} = \text{O}$ stretching (~ 80%) + NH bending (~ 20%)	43
1546	Amide II	Combination N–H in plane bending and C–N stretching	43
1453, 1405	CO_3^{2-}	Asymmetric stretching (ν_3)	17,23,38,43,68–70
1237	Amide III	CN stretching + NH bending (~ 30% each), CC stretching (~ 20%) and CH bending (~ 10%)	43
1101, 1021	PO_4^{3-}	Asymmetric stretching (ν_3)	17,23,38,43,68–70
960	PO_4^{3-}	Symmetric stretching (ν_1)	
870	CO_3^{2-}	Symmetric bending (ν_2)	
601, 575, 562	PO_4^{3-}	Asymmetric bending (ν_4)	
470	PO_4^{3-}	Symmetric bending (ν_2)	

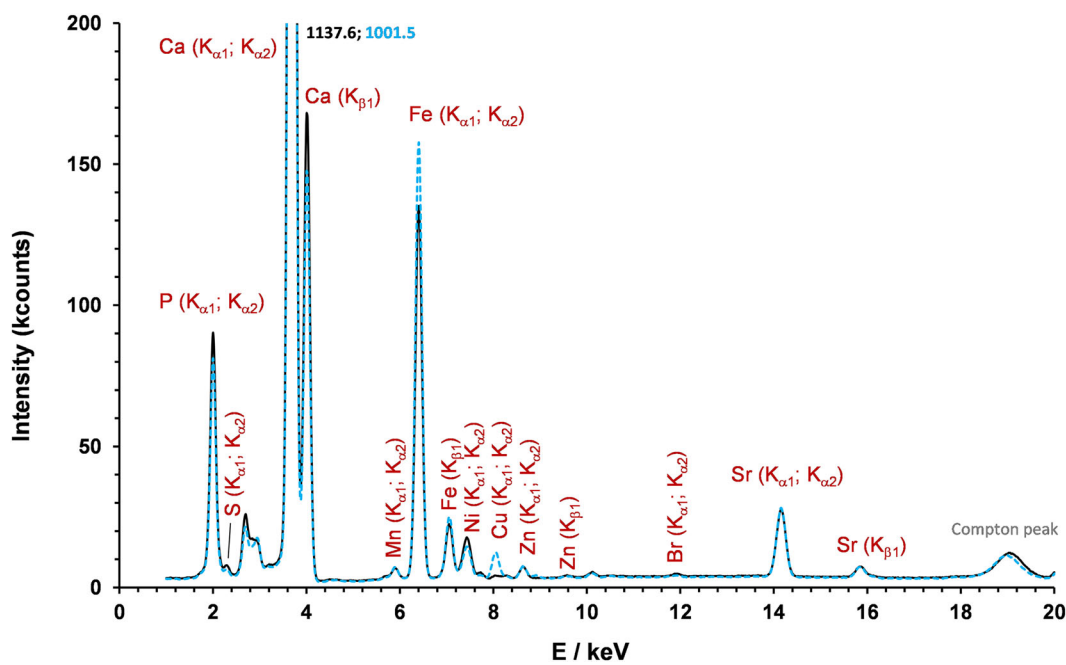


Fig. 4 | Representative XRF spectra of ivory samples: Sample PHA (black continuous line) and sample BHA_34 (blue dotted line). Main elements detected and corresponding lines. Peaks from elements present in the instrument, atmosphere, sum/pile-up peaks and escape peaks were not analysed. XRF conditions were

accelerating voltage and current, 40.00 kV and 30.00 mA using an X-ray tube with Rhodium anode; Acquisition time: 180 s; No filter; No vacuum. Since no peak of analytical interest was observed in any of the samples above 20 keV (only rhodium and palladium peaks from Tracer), only the energy range 1–20 keV is displayed.

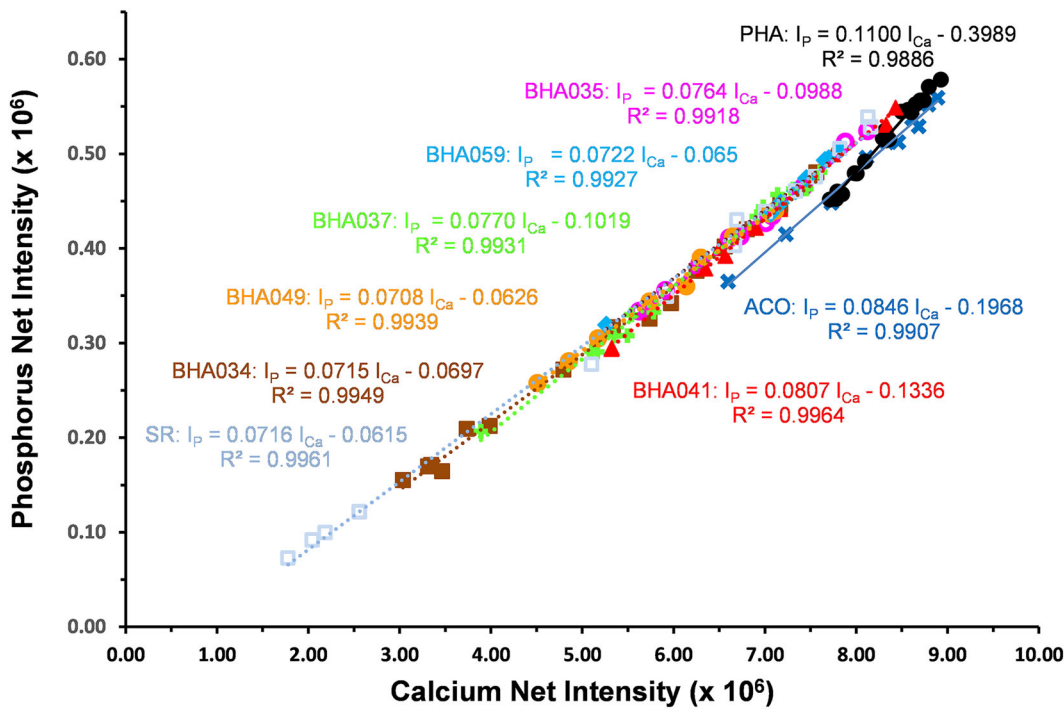


Fig. 5 | Bivariate plot of phosphorous and calcium net intensities for the nine ivory samples and respective regression analysis. Each sample is represented by a colour, indicated in the points on the chart.

ferent spots of a same piece, the net intensities of Ca and P peaks varied, ranging approximately from 1.5×10^6 to 9.0×10^6 intensity units for Ca, and from 0.1×10^6 to 0.6×10^6 intensity units for P, due to matrix effects (non-constant density, non-uniform element distribution and analyte radiation interaction with other atoms) or geometric factors (uneven analysis spots and variable distance between the surface of samples and XRF detector). Even though, P fluorescence is more prone to suffer attenuation effects than Ca, and Ca enrichment and P loss can occur in marine environments²¹, it was possible to report a good correlation between the net intensities of both elements for the spectra analysed (Fig. 5).

In fact, seven of these samples presented a similar correlation between the net intensities of both elements, while sample ACO and sample PHA, present a slightly different correlation, most probably, due to their matrix structure. Regarding the other two major elements, Fe and Sr, while the signal from Fe varies considerably between samples, the Sr signal varies less along the heterogeneity of the sample. In elephant ivory, Fe is not considered a major element but is frequently detected by X-ray fluorescence and other techniques, either in modern items^{25,49} or in buried or submerged ivories^{17,21}. In addition, some part of the detectable Fe in these archaeological items can result from antemortem biogenesis processes occurring during the elephant tusks development²⁷. However, the high detection levels, suggests a prevalence of postmortem diagenesis contamination processes occurring during the prolonged exposure of the ivory items on iron-rich natural minerals from the surrounding seabed environment or from the corrosion of iron artefacts. In fact, the detection of the other elements can also be interpreted in a similar way, as noted in other studies^{50,51}. The presence of Sr in the ivory tusks can also be attributed to diagenetic origin¹⁷ and, in less extend to biogenic causes, such as the local diet of elephants⁵². Sr is frequently detected in several ivory items including being used to discover its geographic provenance based on the local diet of elephants⁵². Moreover, Sr, among others (e.g. Zn), competes biologically with Ca, by occupying the same ionic transporters and binding sites in the hydroxyapatite matrix⁵³. The absence of Sr detection may be due to its very low concentration in ivory (lower than the limit of detection of the analytical instrument) or linked to a diet low in strontium compounds. As reported by Buddhachat et al.²⁵, not detecting Sr is not necessarily be due to the use of a handheld XRF unit

operating at an accelerating voltage of 50 kV. Sr concentration below the instrument's detection limit, matrix-induced attenuation of Sr fluorescence, spectral overlap with adjacent peaks, variable measurement geometry, or insufficient acquisition time, rather than the accelerating voltage itself. Considering that the K-edge for strontium is 16.1 keV, numerous examples in the literature demonstrate that detection is achievable at lower accelerating voltages, such as the 40 kV⁵⁴⁻⁵⁶.

Copper exhibited markedly different characteristics in samples PHA and ACO compared to the other seven samples analysed. In PHA and ACO, copper was below the detection limit, whereas it was clearly detectable in the remaining samples. Given that all specimens were subjected to the same marine depositional environment for an equivalent duration and were analysed under identical laboratory conditions, diagenetic alteration is unlikely to account for this discrepancy in copper detection. This observation supports the hypothesis that the copper detected in the seven samples is of biogenic origin, having been incorporated into the skeletal tissues during the life of the organism. Conversely, the absence of copper in PHA and ACO suggests that these individuals may have belonged to a biologically distinct group from that represented by the remaining samples. Further evidence for this distinction is provided by the correlation patterns between the net intensities of phosphorus (P) and calcium (Ca). The seven copper-bearing samples exhibit consistent P/Ca relationships, which differ significantly from those observed in the PHA and ACO samples. Together, these findings point to the existence of two distinct biological groups, characterized by differing elemental compositions, possibly reflecting taxonomic or ecological divergence among the individuals analysed (Fig. 5). The remaining elemental data are insufficient to clearly distinguish between samples and do not support any reliable inference regarding the geographic origin of the elephants.

Lastly, we re-evaluated the role attributed to hafnium (Hf) as a discriminant element between African and Asian elephant ivory, as previously suggested by Singh et al.²². Although these authors employed WDXRF in combination with ICP-AES and ICP-MS, Hf was not detected by the latter two techniques, and no explanation was provided for this discrepancy, this lack of analytical confirmation introduced uncertainty regarding the reliability of Hf as a geographic marker.

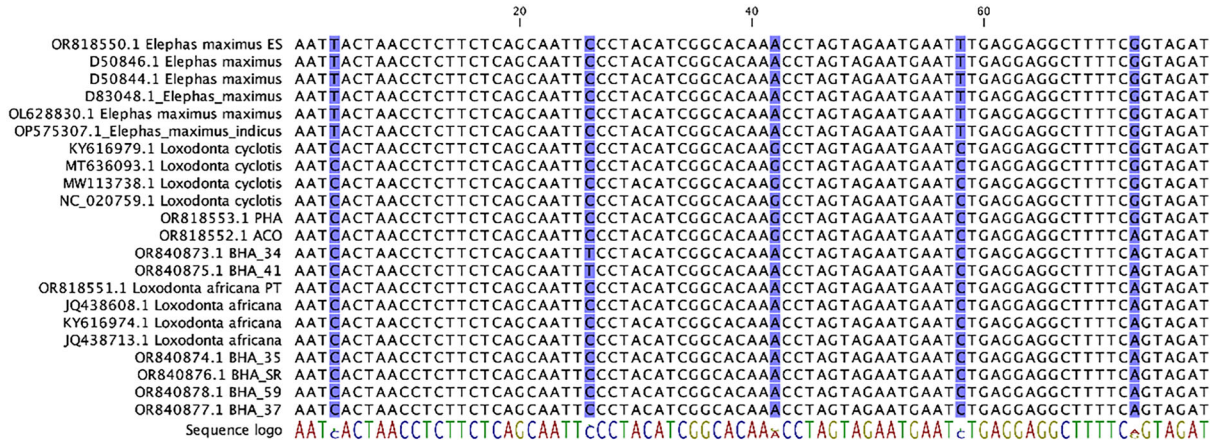


Fig. 6 | Alignment for elephant ivory and stool obtained for short 79 bp amplicon of cyt (b).

Furthermore, Kautenburger et al.⁴⁹ who analysed a larger and more diverse set of ivory samples using WDXRF, also did not report the presence of Hf. To our knowledge, no other published studies confirmed the presence of this element in either African or Asian ivory. Based on our own measurements and instrument setup, we suggested that the peak assigned to Hf in Singh et al.²² may have corresponded to second-order reflections of strontium (Sr) transitions. Specifically, when using a LIF 200 crystal ($2d = 4.026 \text{ \AA}$), the Sr $K\beta_1$ (15.836 keV) and $K\beta_3$ (15.826 keV) transitions produced second-order reflections at $2\theta \approx 45.77$ and 45.80, respectively, values that closely coincided with the Hf La_1 transition at $2\theta = 45.88$ (7.899 keV).

This type of spectral overlap was a known phenomenon in WDXRF. For instance, Afzal et al.⁵⁷ demonstrated that the Zr $K\alpha$ line (15.78 keV) produced a second-order reflection at $2\theta = 45.93$ when using a LIF 100 crystal, potentially leading to similar misinterpretations. Additionally, the spectra presented by Singh et al.²², did not show other primary Hf peaks (e.g., at 46.22° or $39.91^\circ 2\theta$), which further complicated confident identification of this element. Taken together, these observations called for a cautious interpretation of Hf signals in ivory analyses using WDXRF, especially when spectral interferences were not explicitly addressed.

Molecular identification of ivory tusks

Ancient DNA methods have identified elephant ivory sources in several studies. De Flamingh et al.⁹ used DNA analysis to confirm that the over 100 tusks on the “Bom Jesus” shipwreck belonged to forest elephants from the Guinean and Congolese forests in eastern and central Africa. Earlier, Lee et al.⁵⁸ developed a method to differentiate elephant species for conservation, and Comstock et al.⁵⁹ described a technique to isolate and amplify genomic and mitochondrial DNA from African ivory using minimal amount of ivory. Another study by Lee et al.⁶⁰ analysed black-market ivory, identifying nine samples by species and origin.

Working with ancient DNA of ivory tusks is a highly challenging task, mostly due nature of the material and its preservation conditions^{58,61}. For DNA profiling in this research, all samples (ivory and control faeces) underwent sequencing of a 116 bp mitochondrial *cyt b* gene fragment to amplify elephant DNA while excluding non-elephant species and avoiding human contamination²⁹. Due to the high fragmentation level of the DNA extracted, expected in this type of material, this short fragment was selected for the identification of the elephant species and geographical origin of the ivory samples. This marker has been demonstrated to be sufficient to distinguish elephantid DNA from other sources, and efficient for degraded DNA from ancient ivory²⁹.

The high concentration of Ca in these samples is usually reduced by a demineralization step with EDTA^{28,62–64}. The presence of this chelating agent can interfere negatively in downstream molecular applications⁶⁵. In this sense, the additional cleaning-step with EDTA was crucial for the extraction

of amplifiable DNA on this type of material. Briefly, EDTA will form a metal complex with the Ca present in the ivory samples, and after removing the complex formed an additional washing step with a magnesium nitrate solution is performed to remove, also by metal chelation, the remaining EDTA. Taking advantage of the fact that the two metal cations form sufficiently stable complexes with EDTA (e.g., in determining water hardness)⁶⁶, to our knowledge, this is the first study to emphasize the importance of removing EDTA as a contaminating agent and, ultimately, improving DNA availability for extraction and subsequent procedures, without any deleterious effect of the magnesium ion.

To our knowledge, this is the first study to stress the importance of removing EDTA as a contamination agent and ultimately improve the DNA availability for extraction and following procedures.

From the nine ivory samples, only eight were successfully amplified, together with the control samples from African savanna (*L. africana* PT) and Asian elephants (*E. maximus* ES). The obtained sequences were aligned with mitochondrial sequences of *L. africana*, *L. cyclotis* and *E. maximus* (Fig. 6). A total of four polymorphic sites were identified in the highly conservative sequence of *cyt b*. Overall, African species, *L. africana* and *L. cyclotis*, presented two nucleotide polymorphisms, A→C (position 42 of the alignment) and G→A (position 73), while to distinguish African from the Asian species (*E. maximus*, *E. maximus maximus*, and *E. maximus indicus*), 3 polymorphic sites were detected (T→C; A→G; G→A) (Fig. 6).

All ivory samples from BHA-001 were identified as African elephants (Fig. 7). A clear separation between Asian elephants (*E. maximus*) and African elephants is observed with a good bootstrap support. Within the African clade, two sub-clades can be observed, the sub-clade of African forest elephants *L. cyclotis* with PHA sample grouped, and the sub-clade of African savanna elephants, *L. africana*, clustering the other ivory samples. Mondol et al.⁶⁷ has proven the existence of two divergent clades of mtDNA, the clade of only savanna elephant (S clade) and the clade of forest elephants and sometimes some savanna elephants (F clade). This may help to explain the PHA positioning closer to *L. cyclotis*. However, according to Ngatia et al.²⁹, the mtDNA marker designed can only identify savanna elephants and not assign forest elephants or hybrid species without other nuclear markers. It's of interest to note that sample ACO, like PHA, belongs to a different lineage of African elephants. This divergence may correlate with their elemental composition, as both samples showed copper levels below the detection limit, whereas Cu was detectable in the other samples. It raises the possibility that dietary or ecological variables may be reflected in variations in trace element composition.

Discussion

Among the various objectives outlined for this study, it was possible to determine the African origin of the ivory collection from BH-001, possibly being acquired during a stopover at an African port, strengthening the

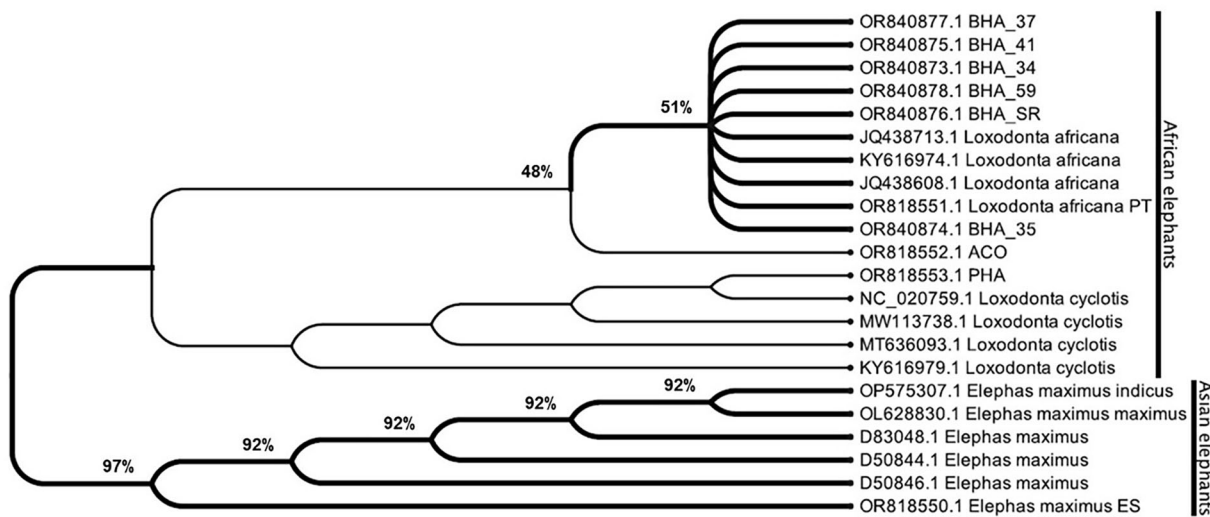


Fig. 7 | Maximum likelihood phylogenetic tree of the short fragment of the cytochrome b (Ctyb) sequence data. Clades were highlighted and formed with bootstrap threshold higher than 50%.

working hypothesis initially put forward by archaeological research. To achieve this specific objective, ancient DNA (aDNA) analysis was used, while a DNA extraction procedure was developed in parallel, which favourably amplifies its detection. The study underlines the importance of combining multiple analytical techniques for a comprehensive understanding of ivory, recognizing the limitations and challenges posed by environmental factors and sample age.

Knowing that the chance to amplify aDNA correlates strongly with the preservation of ivory constituents, particularly with changes in its mineral and organic components, the ATR-FTIR technique, with well-known merits in the characterization of materials of osteological nature, was used to assess whether aDNA analysis was a viable option and to gain a clearer understanding of the preservation of structural and chemical properties of archaeological ivories in a marine context. Both ATR-FTIR and XRF are simple, fast, and non-destructive analytical techniques that enable the examination of valuable archaeological materials without causing damage.

The remarkable dependence of the carbonate, phosphate, and amide band intensities in the FTIR spectra on the preservation state of the samples, and the evaluation of the corresponding indicators of crystallinity and preservation, proved very useful in discriminating samples with different preservation states (i.e., less altered/diagenetically stable from highly degraded ones). The results indicate that the degradation of the ivory in the identified marine context is not severe, suggesting good preservation of the dentin matrix and, consequently, the potential survival of ancient DNA.

This interpretation is corroborated by XRF analysis. Although some differences were observed in the elemental composition of the samples, either due to environmental contamination caused by other artifacts from the shipwreck or due to natural variability among elephant tusks (for instance, in two of the samples, PHA and ACO, no copper was detected), all samples present an elemental composition typical of elephant ivory. In line with other studies using XRF analysis to characterize and distinguish ivory from elephants raised in different environments, our findings point to the existence of two distinct biological groups.

On a broader perspective, the study underlines the importance of combining multiple analytical techniques for a comprehensive understanding of ivory, recognizing the limitations and challenges posed by environmental factors and sample age. This investigation contributed to the knowledge of underwater heritage, providing valuable insights into the genetic and elemental composition of ancient ivory, offering considerations for future studies. From an archaeological point of view, the African origin of the ivory cargo from the BH-001 shipwreck has opened research perspectives of interest on multiple scales. In the context of Atlantic navigation, this

result confirms that BH-001 was involved in the maritime trade between Africa and Europe in the first quarter of the 18th century. The ivory trade was conducted on a large scale via the “triangular route”, which connected Europe to Africa in the first stage, Africa to America in a second, and then the American continent to Europe. The main purpose of this route was to supply the European colonies on the American continent with African slaves, who were used on sugar and tobacco plantations. This topic of research has attracted the interest of underwater archaeologists in recent decades due to the social, political, and cultural impact of the slave trade. It is also known that ships from the African continent arrived in the Azores to make technical stopovers, regardless of their destination. The possible connection between BH-001 and these routes places the Azores at the centre of the debate on the role of the Azores islands in the Atlantic economy of the 18th century.

Data availability

Cytochrome b sequences generated in this study were deposited under the accessions OR818550-OR818553 and OR840873-OR840878.

Received: 22 September 2025; Accepted: 30 November 2025;

Published online: 19 December 2025

References

1. Bettencourt, J. Shipwrecks in the azores and global navigation (sixteenth to nineteenth centuries): an overview. *Int. J. Histor. Archaeol.* **28**, 895–926 (2024).
2. Cascalheira, J. & Gonçalves, C. Proceedings of the 4th Young Researchers in Archaeology Conference – JIA 2011 Vol. II. [Actas das IV Jornadas de Jovens em Investigação Arqueológica – JIA 2011 Vol. II] (in Portuguese). *Núcleo de Arqueologia e Paleoecologia e Departamento de Artes e Humanidades, Faculdade de Ciências Humanas e Sociais, Universidade do Algarve, Faro* (2011).
3. Neto, J. L., Bettencourt, J., Borges, L. & Parreira, P. Strategies for the Promotion of Underwater Cultural Heritage in the Azores: The Case of Faial Island. [Estratégias de promoção do património cultural subaquático nos Açores. O caso da ilha do Faial] (in Portuguese). *In Arqueologia em Portugal 2020 – Estado da Questão – Textos* **298**, (2020).
4. Bettencourt, J. The Azores in Global Navigation: The Contribution of Underwater Archaeology. [Os Açores Na Navegação Global: O Contributo Da Arqueologia Subaquática] (in Portuguese). *Boletim do Núcleo Cultural da Horta* 307–342 (2017).

5. Bettencourt, J. & Carvalho, P. The Submerged History in the Bay of Horta: Preliminary Results of the Archaeological Work on the “Ivory Shipwreck” (First Quarter of the 18th Century). [A História Submersa Na Baía Da Horta: Resultados Preliminares Dos Trabalhos Arqueológicos No “Naufrágio Do Marfim” (Primeiro Quartel Do Século XVIII)] (in Portuguese). *Academia.edu* (2010).
6. Pearce, J. Clay tobacco pipes made by the Manby family of London. *Soc. Clay Pipe Res. Newsletter* **6**, 71–82 (2013).
7. Bertoglio, B. Bone tissue preservation in seawater environment: a preliminary comparative analysis of bones with different post-mortem histories through anthropological and radiological perspectives. *Int. J. Legal Med.* **135**, 2581–2594 (2021).
8. Bettencourt, J. The Port of Horta in the History of the Atlantic (16th–20th Centuries) from the Archaeological Record: Some Examples. [O porto da Horta na História do Atlântico (sécs. XVI a XX) a partir do registo arqueológico: alguns exemplos] (in Portuguese). In *O Reencontro com o mar no Século XXI* (2012).
9. de Flamingh, A. et al. Sourcing elephant ivory from a sixteenth-century Portuguese shipwreck. *Curr. Biol.* **31**, 621–628.e4 (2021).
10. Herry, N. Report on finds from the Saint-Quay-Portrieux wreck, France. *Int. J. Naut. Archaeol.* **33**, 96–105 (2004).
11. Moore, D. D. & Malcom, C. Seventeenth-century vehicle of the middle passage: archaeological and historical investigations on the Henrietta Marie shipwreck site. *Int. J. Histor. Archaeol.* **12**, 20–38 (2008).
12. Tripati, S. & Godfrey, I. Studies on elephant tusks and hippopotamus teeth collected from the early 17th century Portuguese shipwreck off Goa, west coast of India: evidence of maritime trade between Goa, Portugal and African countries. *Curr. Sci.* **92**, 332–339 (2007).
13. Chirikure, S., Sinamai, A., Goagoses, E., Mubusisi, M. & Ndoro, W. Maritime archaeology and trans-oceanic trade: a case study of the Oranjemund shipwreck cargo, Namibia. *J. Mar. Archaeol.* **5**, 37–55 (2010).
14. Hauptmann, A., Schneider, G. & Bartels, C. The shipwreck of Bom Jesus, AD 1533: Fugger Copper in Namibia. *J. Afri. Archaeol.* **14**, 184–207 (2016).
15. Tripati, S. & Gaur, A. S. Exploration of a Portuguese shipwreck in Goa waters, western coast of India. *Bullet. Aust. Inst. Maritime Archaeol.* **30**, 127–136 (2006).
16. Dal Sasso, G., Asscher, Y., Angelini, I., Nodari, L. & Artioli, G. A universal curve of apatite crystallinity for the assessment of bone integrity and preservation. *Sci. Rep.* **8**, 12025 (2018).
17. Godfrey, I. M., Ghisalberti, E. L., Beng, E. W., Byrne, L. T. & Richardson, G. W. The analysis of ivory from a marine environment. *Stud. Conserv.* **47**, 29–45 (2002).
18. Ábelová, M. Schreger pattern analysis of *Mammuthus primigenius* tusk: analytical approach and utility. *Bull. Geosci.* **83**, 225–232 (2008).
19. Trapani, J. & Fisher, D. C. Discriminating proboscidean taxa using features of the Schreger pattern in Tusk Dentin - ScienceDirect. *J. Archaeol. Sci.* **30**, 429–438 (2003).
20. Espinoza, E. O. & Mann, M.-J. The history and significance of the Schreger pattern in Proboscidean Ivory Characterization. *J. Am. Inst. Conserv.* **32**, 241–248 (1993).
21. Doménech-Carbó, M. T., Buendía-Ortuño, M., Pasies-Oviedo, T. & Osete-Cortina, L. Analytical study of waterlogged ivory from the Bajo de la Campana site (Murcia, Spain). *Microchem. J.* **126**, 381–405 (2016).
22. Singh, R. R., Goyal, S. P., Khanna, P. P., Mukherjee, P. K. & Sukumar, R. Using morphometric and analytical techniques to characterize elephant ivory. *Forensic Sci. Int.* **162**, 144–151 (2006).
23. Wang, K. et al. FTIR study on the phase transition of experimental and archaeological burnt ivory. *Herit. Sci.* **10**, 131 (2022).
24. Ziegler, S., Merker, S., Streit, B., Boner, M. & Jacob, D. E. Towards understanding isotope variability in elephant ivory to establish isotopic profiling and source-area determination. *Biol. Conserv.* **197**, 154–163 (2016).
25. Buddhachat, K. et al. Use of handheld X-ray fluorescence as a non-invasive method to distinguish between Asian and African elephant tusks. *Sci. Rep.* **6**, 24845 (2016).
26. McLellan, M. J., Carrothers, K. L. & Spicer, A. M. Investigating the utility of a handheld X-ray fluorescence (XRF) device as a field test for suspected ivory. *Forensic Sci. Int. Animals Environ.* **2**, 100041 (2022).
27. Espinoza, E. O. Identification of ivory using a handheld XRF spectrometer. *Int. J. Forensic Sci. Crim.* **8**, 1–10 (2023).
28. Xavier, C. et al. Evaluation of DNA extraction methods developed for forensic and ancient DNA applications using bone samples of different age. *Genes (Basel)* **12**, 146 (2021).
29. Ngatia, J. N., Lan, T. M. & Ma, Y. Distinguishing extant elephants ivory from mammoth ivory using a short sequence of cytochrome b gene. *Sci. Rep.* **9**, 18863 (2019).
30. Dagona, A. G. (56) BioEdit: a user-friendly biological sequence alignment editor and analysis program for Windows 95/98/NT. *Nucleic Acids Symp. Ser.* **41**, 95–98 (1999).
31. Katoh, K. & Standley, D. M. MAFFT multiple sequence alignment software version 7: improvements in performance and usability. *Mol. Biol. Evol.* **30**, 772–780 (2013).
32. Capella-Gutiérrez, S., Silla-Martínez, J. M. & Gabaldón, T. trimAl: a tool for automated alignment trimming in large-scale phylogenetic analyses. *Bioinformatics* **25**, 1972–1973 (2009).
33. Bridge, J. & Demicco, R. *Earth Surface Processes, Landforms and Sediment Deposits* (Cambridge University Press, Cambridge, 2008).
34. Kendall, C., Eriksen, A. M. H., Kontopoulos, I., Collins, M. J. & Turner-Walker, G. Diagenesis of archaeological bone and tooth. *Palaeogeogr. Palaeoclimatol. Palaeoecol.* **491**, 21–37 (2018).
35. Beasley, M. M., Bartelink, E. J., Taylor, L. & Miller, R. M. Comparison of transmission FTIR, ATR, and DRIFT spectra: implications for assessment of bone bioapatite diagenesis. *J. Archaeol. Sci.* **46**, 16–22 (2014).
36. France, C. A. M., Sugiyama, N. & Aguayo, E. Establishing a preservation index for bone, dentin, and enamel bioapatite mineral using ATR-FTIR. *J. Archaeol. Sci. Rep.* **33**, 102551 (2020).
37. Jose, S. A. et al. Development of FTIR spectral library for the identification of Asian elephant ivory: an innovative approach in wildlife forensics. *Discov. Appl. Sci.* **6**, 1–16 (2024).
38. Wang, L. et al. Infrared spectroscopic study of modern and ancient ivory from sites at Jinsha and Sanxingdui, China. *Mineral. Mag.* **71**, 509–518 (2007).
39. Albéric, M. et al. Early diagenesis of elephant tusk in marine environment. *Palaeogeogr. Palaeoclimatol. Palaeoecol.* **416**, 120–132 (2014).
40. Edwards, H. G. M., Farwell, D. W., Holder, J. M. & Lawson, E. E. Fourier transform-Raman spectroscopy of ivory: a non-destructive diagnostic technique. *Stud. Conserv.* **43**, 9 (1998).
41. Loy, C., Brock, F. & Dyer, C. Investigating diagenesis of archaeological bones from Etton Causewayed enclosure. *UK. Quat. Int.* **660**, 21–30 (2023).
42. Scaggion, C. et al. An FTIR-based model for the diagenetic alteration of archaeological bones. *J. Archaeol. Sci.* **161**, 105900 (2024).
43. Stani, C., Vaccari, L., Mitri, E. & Birarda, G. FTIR investigation of the secondary structure of type I collagen: new insight into the amide III band. *Spectrochim. Acta A Mol. Biomol. Spectrosc.* **229**, 118006 (2020).
44. Sun, X., He, M. & Wu, J. Crystallographic characteristics of inorganic mineral in mammoth ivory and ivory. *Minerals* **12**, 117 (2022).
45. Banerjee, A., Bortolaso, G. & Dindorf, W. *Distinction Between African and Asian Ivory. [Elfenbein und Artenschutz] (in German)* (Bundesamt für Naturschutz, 2008).
46. Nocete, F., Vargas, J. M., Schuhmacher, T. X., Banerjee, A. & Dindorf, W. The ivory workshop of Valencina de la Concepción (Seville, Spain) and the identification of ivory from Asian elephant on the Iberian

Peninsula in the first half of the 3rd millennium BC. *J. Archaeol. Sci.* **40**, 1579–1592 (2013).

47. Rozalen, M. & Ruiz Gutierrez, A. A study of the origin and gilding technique of a Hispano-Philippine ivory from the XVIth century. *J. Archaeol. Sci. Rep.* **4**, 1–7 (2015).

48. Bajnóczki, B., Koncz, I. & Bollók, Á. Tracing the road of elephant ivory at the end of Late Antiquity—Archaeometric analysis of ivory artefacts from the 6th–7th-century Carpathian Basin. *Acta Archaeol.* **74**, 399–414 (2023).

49. Kautenburger, R., Wannemacher, J. & Müller, P. Multi element analysis by X-ray fluorescence: a powerful tool of ivory identification from various origins. *J. Radioanal. Nucl. Chem.* **260**, 399–404 (2004).

50. Sponheimer, M. Alteration of enamel carbonate environments during fossilization. *J. Archaeol. Sci.* **26**, 143–150 (1999).

51. Willmes, M. et al. Improvement of laser ablation *in situ* micro-analysis to identify diagenetic alteration and measure strontium isotope ratios in fossil human teeth. *J. Archaeol. Sci.* **70**, 102–116 (2016).

52. Hemer, K. A., Willmott, H., Evans, J. E. & Buckley, M. Ivory from early Anglo-Saxon burials in Lincolnshire—a biomolecular study. *J. Archaeol. Sci. Rep.* **49**, 103943 (2023).

53. Prozesky, V. M. et al. Trace element concentration and distribution in ivory. *Nucl. Instrum. Methods Phys. Res. B* **104**, 638–644 (1995).

54. Byrnes, J. F. & Bush, P. J. Practical considerations in trace element analysis of bone by portable X-ray fluorescence. *J. Forensic Sci.* **61**, 1041–1045 (2016).

55. Specht, A. J., Mostafaei, F., Lin, Y., Xu, J. & Nie, L. H. Measurements of strontium levels in human bone *in vivo* using portable x-ray fluorescence (XRF). *Appl. Spectrosc.* **71**, 1962–1968 (2017).

56. Zhang, X. et al. *In vivo* quantification of strontium in bone among adults using portable x-ray fluorescence. *J. Trace Elem. Med. Biol.* **74**, 127077 (2022).

57. Afzal, M., Hanif, J., Hanif, I., Qadeer, R. & Saleem, M. Determination of zirconium and hafnium in solution by X-ray fluorescence spectrometry: a practical approach. *J. Radioanal. Nucl. Chem.* **139**, 203–214 (1990).

58. Lee, J. C.-I. et al. Ivory identification by DNA profiling of cytochrome b gene. *Int. J. Legal Med.* **123**, 117–121 (2009).

59. Comstock, K. E., Ostrander, E. A. & Wasser, S. K. Amplifying nuclear and mitochondrial DNA from African Elephant Ivory: a tool for monitoring the ivory trade. *Conserv. Biol.* **17**, 1840–1843 (2003).

60. Lee, E. et al. The identification of elephant ivory evidences of illegal trade with mitochondrial cytochrome b gene and hypervariable D-loop region. *J. Forensic Leg. Med.* **20**, 174–178 (2013).

61. Aznar-Cormano, L., Bonnald, J., Krief, S., Guma, N. & Debruyne, R. Molecular sexing of degraded DNA from elephants and mammoths: a genotyping assay relevant both to conservation biology and to paleogenetics. *Sci. Rep.* **11**, 7227 (2021).

62. Ewart, K. M. et al. Expediting the sampling, decalcification, and forensic DNA analysis of large elephant ivory seizures to aid investigations and prosecutions. *Forensic Sci. Int. Gen.* **44**, 102187 (2020).

63. Hale, C. et al. Investigating the origins of ivory recovered in the United Kingdom. *Forensic Sci. Int. Animals Environ.* **1**, 100027 (2021).

64. Mailand, C. & Wasser, S. K. Isolation of DNA from small amounts of elephant ivory. *Nat. Protoc.* **2**, 2228–2232 (2007).

65. Nkuna, R., Ijoma, G. N. & Matambo, T. S. Applying EDTA in chelating excess metal ions to improve downstream DNA recovery from mine tailings for long-read amplicon sequencing of acidophilic fungi communities. *J. Fungi* **8**, 419 (2022).

66. Skoog, D. A., West, D. M., Holler, F. J. & Crouch, S. R. *Fundamentals of Analytical Chemistry* (Cengage, Australia Brazil, 2022).

67. Mondol, S. et al. New evidence for hybrid zones of forest and savanna elephants in Central and West Africa. *Mol. Ecol.* **24**, 6134–6147 (2015).

68. Chang, M. C. & Tanaka, J. FT-IR study for hydroxyapatite/collagen nanocomposite cross-linked by glutaraldehyde. *Biomaterials* **23**, 4811–4818 (2002).

69. Li, X. et al. Fourier-transformed infrared spectroscopy study of the ancient ivory tusks from the Sanxingdui site. *Front. Earth Sci.* **10**, 1–10 (2023).

70. Padilla, S., Izquierdo-Barba, I. & Vallet-Regí, M. High specific surface area in nanometric carbonated hydroxyapatite. *Chem. Mater.* **20**, 5942–5944 (2008).

Acknowledgements

The authors would like to thank Lisbon Zoo (Jardim Zoológico de Lisboa, Portugal) and Terra Natura Benidorm Zoo (Benidorm, Spain) for kindly providing the samples of different elephant species.

Author contributions

M.C. performed the sample analyses using all methodologies, analysed the data, and wrote the manuscript. C.V. and M.E. were responsible for DNA analyses and contributed to manuscript writing. J.M.S.F. assisted in writing, reviewing, and editing the manuscript. J.G.T. analysed the data from XRF and FTIR analyses and contributed to manuscript writing. J.B. provided the archaeological samples and the historical context for the manuscript. D.M.T. supervised the work, participated in reviewing and editing, and contributed to manuscript writing. All authors reviewed the manuscript.

Competing interests

The authors declare no competing interests.

Additional information

Supplementary information The online version contains supplementary material available at <https://doi.org/10.1038/s40494-025-02245-1>.

Correspondence and requests for materials should be addressed to Dora Martins Teixeira.

Reprints and permissions information is available at <http://www.nature.com/reprints>

Publisher's note Springer Nature remains neutral with regard to jurisdictional claims in published maps and institutional affiliations.

Open Access This article is licensed under a Creative Commons Attribution-NonCommercial-NoDerivatives 4.0 International License, which permits any non-commercial use, sharing, distribution and reproduction in any medium or format, as long as you give appropriate credit to the original author(s) and the source, provide a link to the Creative Commons licence, and indicate if you modified the licensed material. You do not have permission under this licence to share adapted material derived from this article or parts of it. The images or other third party material in this article are included in the article's Creative Commons licence, unless indicated otherwise in a credit line to the material. If material is not included in the article's Creative Commons licence and your intended use is not permitted by statutory regulation or exceeds the permitted use, you will need to obtain permission directly from the copyright holder. To view a copy of this licence, visit <http://creativecommons.org/licenses/by-nc-nd/4.0/>.

© The Author(s) 2025